Turnover Rates of B Cells, T Cells, and NK Cells in Simian Immunodeficiency Virus-Infected and Uninfected Rhesus Macaques[1]

Rob J. De Boer,[2]* Hiroshi Mohri,[†] David D. Ho,[†] and Alan S. Perelson[‡]

We determined average cellular turnover rates by fitting mathematical models to 5-bromo-2′-deoxyuridine measurements in SIV-infected and uninfected rhesus macaques. The daily turnover rates of $CD4^+$ T cells, $CD4^-$ T cells, $CD20^+$ B cells, and $CD16^+$ NK cells in normal uninfected rhesus macaques were 1, 1, 2, and 2%, respectively. Daily turnover rates of $CD45RA^-$ memory T cells were 1%, and those of $CD45RA^+$ naive T cells were 0.5% for $CD4^+$ T cells and ~1% for $CD4^-CD45RA^+$ T cells. In SIV-infected monkeys with high viral loads, the turnover rates of T cells were increased ~2-fold, and that of memory T cells ~3-fold. The turnover of $CD4^+CD45RA^+$ naive T cells was increased 2-fold, whereas that of $CD4^-CD45RA^+$ naive T cells was marginally increased. B cells and NK cells also had increased turnover in SIV-infected macaques, averaging 3 and 2.5% per day, respectively. For all cell types studied here the daily turnover rate increased with the decrease of the CD4 count that accompanied SIV infection. As a consequence, the turnover rates of $CD4^+$ T cells, $CD4^-$ T cells, B cells, and NK cells within each monkey are strongly correlated. This suggests that the cellular turnover of different lymphocyte populations is governed by a similar process which one could summarize as "generalized immune activation." Because the viral load and the CD4 T cell count are negatively correlated we cannot determine which of the two plays the most important role in this generalized immune activation. ***The Journal of Immunology*****, 2003, 170: 2479–2487.**

The rates of lymphocyte turnover during health and disease are poorly characterized. This limits our understanding of diseases like rheumatoid arthritis (1, 2) and HIV-infection (3–14) that lead to increased rates of cellular turnover and ultimately to deterioration of the immune system. HIV-1 infection is known to increase the turnover rates of $CD4^+$ and $CD8^+$ T cells (5, 9, 11, 13), and to deplete the populations of naive $CD4^+$ T cells, naive $CD8^+$ T cells, and memory $CD4^+$ T cells (15, 16). Current estimates for the turnover rates of $CD4^+$ and $CD8^+$ T cells vary between 1 and 2% in normal individuals to 1–10% in HIV-1-infected patients (5, 9–13). The reasons for the increased turnover have been disputed widely (3, 4, 11, 13, 17, 18).

One method of quantifying cellular turnover involves labeling dividing cells with the base analog 5-bromo-2′-deoxyuridine (BrdU),[3] which can be administered via drinking water and substitutes for thymidine in newly synthesized DNA. $BrdU^+$ cells can be easily detected by flow cytometry, and BrdU labeling has been widely used to study lymphocyte kinetics in animals (4, 14, 19–29). BrdU data (as depicted, see Fig. 2) can be described with three parameters. One characterizes the slope with which the fraction of labeled cells increases during BrdU labeling, another characterizes the loss rate of labeled cells after BrdU withdrawal, and the last defines the asymptotic fraction of labeled cells that would be approached if BrdU were given indefinitely. In a more methodological companion paper (30), we demonstrated that one can derive various mathematical models that allow one to estimate these three parameters from the data. In particular, we showed that the average turnover rate, which for a population at steady state is defined as the average death rate, is independent of the biological assumptions underlying a set of biologically reasonable mathematical models used for fitting BrdU data (30). In this study, we use one of these models to analyze BrdU labeling curves for a number of different lymphocyte populations.

Materials and Methods

Rhesus monkeys were given BrdU in drinking water for 3 wk and then were studied for another 7 wk, and subpopulations were sorted; the percentage of $BrdU^+$ cells was determined (4). A representative flow profile is depicted in Fig. 1. Bone marrow aspirate was obtained from each monkey at week 3, the end of BrdU labeling, and examined for the efficiency of in vivo BrdU labeling. Myeloid cells, which are proliferating rapidly, were gated in a light scatter panel. As shown in Fig. 1*a*, most of the myeloid cells in bone marrow were BrdU-positive, indicating that BrdU in drinking water was efficiently absorbed from digestive tracts and incorporated into DNA of proliferating cells. Because the relative distribution over the profile hardly changes, the data do not suggest that there is dilution of label in $BrdU^+$ cells. After 3 wk of labeling, lymph node biopsies were performed on each macaque. For each macaque, the percentage of labeled $CD3^+$ T cells in blood was similar to that in the lymph node, suggesting that the kinetics measured in blood are representative of that occurring in the lymphoid tissue. In addition, when deuterated glucose (^{2}H-glucose) labeling was used in humans (31), labeled cells started appearing in the blood within half a day, again suggesting that blood and tissue rapidly reach equilibrium.

To analyze T cell subsets, the $CD3^+CD4^+$ population gated as shown were counted as $CD4^+$ T cells, whereas the $CD3^+CD4^-$ phenotype was used as a "$CD8^+$ T cell marker" (Fig. 1*b*). We also analyzed $CD8^+$ T cells using the $CD3^+CD8^+$ phenotype (data not shown). However, we observed

*Theoretical Biology, Utrecht University, Utrecht, The Netherlands; †Aaron Diamond AIDS Research Center, The Rockefeller University, New York, NY 10016; and ‡Theoretical Division, Los Alamos National Laboratory, Los Alamos, NM 87545

Received for publication January 28, 2002. Accepted for publication December 23, 2002.

The costs of publication of this article were defrayed in part by the payment of page charges. This article must therefore be hereby marked *advertisement* in accordance with 18 U.S.C. Section 1734 solely to indicate this fact.

[1] Portions of the work were done under the auspices of the U.S. Department of Energy. This work was supported by National Institutes of Health Grants AI28433 and RR06555 (to A.S.P.), and AI40387 (to D.D.H.), the Santa Fe Institute through the Joseph P. Sullivan and Jeanne M. Sullivan Foundation, and the Dutch AIDS Foundation (Grant 4025).

[2] Address correspondence and reprint requests to Dr. Rob J. De Boer, Theoretical Biology, Utrecht University, Padualaan 8, 3584 CH Utrecht, The Netherlands. E-mail address: R.J.DeBoer@bio.uu.nl

[3] Abbreviations used in this paper: BrdU, 5-bromo-2′-deoxyuridine, d^{-1}, per day.

0022-1767/03/$02.00

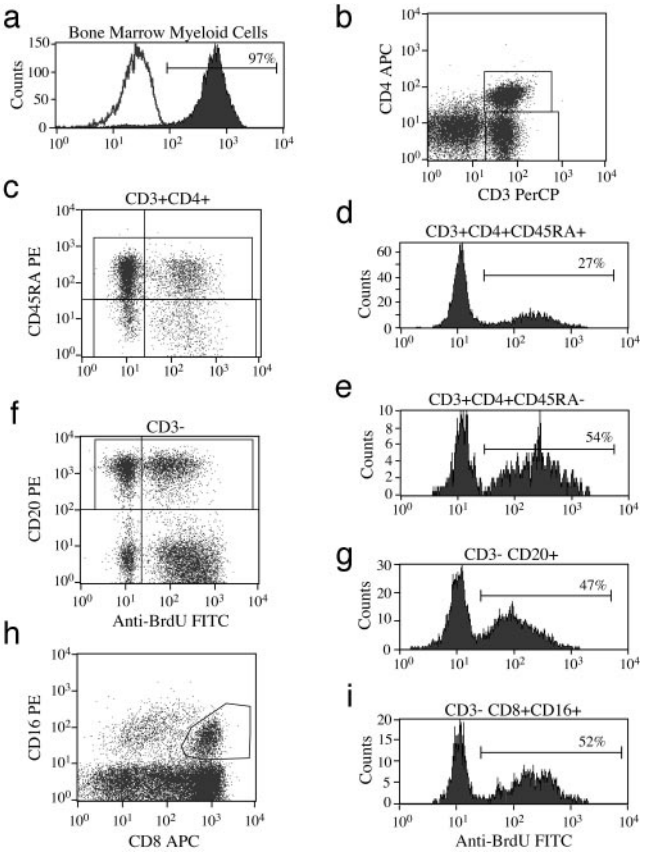

FIGURE 1. Analysis of flow cytometry data. The results from H1316 at week 3 are shown. Staining bone marrow myeloid cells with anti-BrdU Ab or control IgG indicates that most of these rapidly proliferating cells are labeled with BrdU (*a*). To analyze T cell subsets, isolated PBMC were stained with anti-CD3 and anti-CD4 Abs (*b*), together with anti-CD45RA Ab (*c*). CD45RA$^+$ or CD45RA populations in CD3$^+$CD4$^+$ (CD4$^+$ T cells) or CD3$^+$CD4$^-$ (CD8$^+$ T cells) were gated and analyzed for BrdU positivity (*d* and *e*). For B cells, the CD3$^-$CD20$^+$ population was analyzed (*f* and *g*). For NK cells, the CD8$^+$CD16$^+$ population was gated (*h*), and its CD3$^-$ population was analyzed (*i*).

a considerable number of CD4$^+$CD8$^+$ double-positive T cells in some of the monkeys. These CD4$^+$CD8$^+$ double-positive T cells are considered as part of the CD4$^+$ T cell subset. To avoid double counting of those double-positive T cells, we used CD3$^+$CD4$^-$ as a marker of CD8$^+$ T cells due to the instrumental limitation (four-color). Furthermore, anti-CD45RA was used to distinguish between naive (CD45RA$^+$) and memory (CD45RA$^-$) phenotypes (Fig. 1*c*). As shown in Fig. 1, *d* and *e*, memory phenotype had higher incorporation of BrdU than that of naive phenotype in both CD4$^+$ and CD8$^+$ T lymphocytes.

For defining B cells, an anti-CD20 Ab was used, giving a bright signal as shown in Fig. 1*f*. For NK cells, we used the CD3$^-$CD8$^+$CD16$^+$ phenotype as an NK marker. Because CD16 Ag is also expressed on some monocytes, which are highly labeled with BrdU, it is necessary to gate the CD8$^+$CD16$^+$ population very tightly as shown in Fig. 1*h*. NK cells without CD16 expression were, therefore, not included in our study.

We use a simple population dynamical model developed by Mohri et al. (4) and report its parameters by converting them into average turnover rates (30). Briefly, the model considers activated cells, A, that have a source of s cells per day from elsewhere, and which proliferate and die at per cell rates ρ and δ, respectively,

$$dA/dt = s + (\rho - \delta)A. \quad (1)$$

The source could represent 1) the production of cells in the thymus (4), and/or 2) an inflow of activated cells from a compartment of resting cells (29), and/or 3) the large number of progeny of clonally expanded resting or activated cells (30). We will assume that the source yields labeled cells during the labeling period and unlabeled cells thereafter. The latter is required to explain the observed rapid loss of labeled cells after BrdU withdrawal (4, 29, 30). These two assumptions on the presence of labeled cells in the source are consistent with each of the three biological interpretations of the source listed above (Ref. 30; see also *Discussion*). We also allow for a subpopulation of "resting" cells R that hardly pick up BrdU on the time scale of these experiments.

Giving BrdU does not substantially perturb the lymphocyte dynamics, we assume that the various lymphocyte populations remain at steady state throughout the labeling study. Thus, without loss of generality, one can scale the steady state total number of cells to one, i.e., $R + A = 1$. Because at steady state the total number of activated cells remains constant, i.e., $dA/dt = 0$, one obtains for the source $s = (\delta - \rho)A$.

Let L be the fraction of cells labeled with BrdU ($L(0) = 0$), and U the fraction of unlabeled cells. During the labeling period, unlabeled cells are lost by death and by proliferation. Assuming that during the labeling period the source yields labeled cells (30), and that labeling is 100% efficient so that upon division each progeny acquires label, one obtains from equation 1 (4, 29, 30),

$$dL/dt = s + 2\rho U + (\rho - \delta)L, \quad (2)$$

where the two appears once because an unlabeled cell divides into two daughter cells, and division of a labeled cell yields one new labeled cell. Using $s = (\delta - \rho)(1 - R)$ and $U = 1 - L - R$, this has the solution

$$L(t) = \alpha(1 - e^{-(\delta+\rho)t}), \quad (3)$$

where $\alpha = 1 - R$ is the maximum that the fraction of labeled cells would approach if BrdU were given indefinitely. If labeling is $<100\%$ efficient we are overestimating ρ during the labeling period (4, 29). However, the bone marrow aspirations suggested an adequate uptake of BrdU in proliferating cells (Fig. 1).

In the period shortly after BrdU administration has ended, division of labeled cells yields labeled daughter cells (4), because chromosomes with incorporated BrdU are segregated to both daughter cells. However, rapid clonal expansion represented by the source will yield unlabeled cells (30), due to dilution of BrdU to levels that are undetectable (32). Thus, one obtains from equation 1 that

$$dL/dt = (\rho - \delta)L, \quad (4)$$

with the solution

$$L(t) = L(t_e)e^{-(\delta-\rho)(t-t_e)}, \quad (5)$$

where $L(t_e)$ is the fraction of labeled cells at the time, t_e, that BrdU administration ends.

From the model one can easily extract the quantities, $\rho + \delta$, characterizing the initial slope, or up slope, of the labeling curve, $\delta - \rho$ characterizing the rate of decay of labeled cells after labeling has ended, or down slope, and α the asymptote of the labeling curve. Thus, by fitting the model to the data, one can generally estimate the parameters ρ, δ, and α. However, different data sets have particular features which may require variants of this approach. For example, when the up and down slopes $\delta + \rho$ and $\delta - \rho$ are sufficiently similar, one can fit the data with a two parameter model fixing $\rho = 0$. Similarly, whenever the data fail to suggest that a fraction of the cells remains unlabeled one can fit the data with a two parameter model fixing $\alpha = 1$. When both can be fixed one can fit the data with a one parameter model having only δ as a free parameter. Thus, we will fit the data with four models, i.e., the full three parameter "$\alpha\rho\delta$" model, two different two-parameter models, i.e., the "$\alpha\delta$" and the "$\rho\delta$" model, and the one-parameter "δ" variant. For each variant we use the main result of the companion paper (30) and define the average turnover rate as $\hat{\delta} = \alpha\delta$, where $\alpha = 1 - R$ represents the fraction of activated cells, and δ is their rate of turnover. The resting cells are assumed to have a negligible turnover.

In adult monkeys, one expects that naive T cells are largely produced by the thymus and that they have little peripheral proliferation. Thus, for naive T cells the source s would be expected to reflect thymic output, and additionally one expects $\rho \simeq 0$. Because T cell maturation in the thymus follows a "conveyor belt"-type program (33), one expects labeled cells to continue appearing from the thymus after BrdU administration has been stopped. Thus the source of labeled cells is expected to be nonzero for a period of time after BrdU withdrawal. We decided to account for this by making the time at which BrdU administration ends, t_e, a free parameter. This is a correct procedure only in the case $\rho = 0$. Otherwise extending t_e would allow additional labeled cells to be created by proliferation. Thus our "naive T cell model" (see Table III) maximally has three parameters (i.e., α, δ, and t_e).

The main result of the companion paper is that the estimated average turnover rate $\hat{\delta}$ remains very similar if a data set is fitted with any of the

four models outlined above (see Fig. 1 in De Boer et al. (30)). We nevertheless prefer to fit each data set with the most appropriate model. The most appropriate model has sufficient parameters to explain the data, i.e., to allow for a good fit, but at the same time has no redundant parameters that hardly improve the quality of the fit. The quality of a fit is conventionally expressed as the "residual mean square", which is the residual sum of squares divided by the residual degrees of freedom, i.e., the difference between the number of data points and the number of free parameters (34). Thus, although adding a more or less redundant parameter to a model will obviously decrease the residual sum of squares, it will probably increase the residual mean square. Several conventional statistical procedures allow one to select the most appropriate model for a given data set. The partial *F* test compares two nested models by the difference between their residual sum of squares per additional parameter, divided by the residual mean square of the largest of the two models (34). Akaike's Information Criterion is also based on the residual mean square but adds a penalty for the number of parameters (35). Because our estimate for the average turnover rate $\hat{\delta}$ is fairly independent of the precise choice of the model, there is, for our special case, no reason to be conservative with selecting a more complicated model. Therefore, we opted for selecting the model with the lowest residual mean square. Technically, this corresponds to doing a partial *F* test and accepting the more complicated model whenever the *F* value is larger than one. We tested this approach by also doing a somewhat more conservative partial *F* test (i.e., testing whether $F > 1.6$ corresponding to $p < 0.25$). This yielded very similar results: in only 2 of the 120 fits, did we have to pick a simpler model, but as expected (30) we nevertheless obtained very similar estimates for the average turnover $\hat{\delta}$ (not shown).

Parameter estimates were obtained using the DNLS1 subroutine, from the Common Los Alamos Software Library, which is based on the Levenberg-Marquardt algorithm (36) for solving nonlinear least-squares problems. These parameters were used to calculate the predicted T cell population size. Ninety-five percent confidence intervals for the inferred parameters were then determined using a bootstrap method (37), where the residuals to the optimal fit were resampled 500 times.

Results

T cells

Typical examples of the BrdU labeling in $CD4^+$ and $CD4^-$ T cells from an SIV infected and an uninfected macaque are given in Fig. 2, *a* and *b*. The data from the infected monkey were best fitted with the three-parameter $\alpha\rho\delta$ model, and those from the uninfected monkey with the one-parameter δ model. The turnover rate of $CD4^+$ and $CD4^-$ T cells in uninfected rhesus macaques is ~1% per day (Table I). The average turnover rate in SIV-infected macaques with a high viral load is increased ~2-fold, and that in macaques with a low viral load is increased ~1.5-fold. This confirms the previous interpretation of these data that SIV infection increases the cellular turnover in both $CD4^+$ and $CD4^-$ T cells (4), but in this study the average increase remains <2-fold. Although the increase in the turnover rate is relatively small, these results are statistically significant because there is hardly any overlap in the average turnover rates of CD4 and CD8 cells in highly infected and uninfected macaques. An estimated 2-fold increase in cellular turnover of $CD4^+$ T cells is in good agreement with some human data (5), but is lower than other human data (11, 13). Our estimated 2-fold increase in the turnover of $CD8^+$ T cells is also lower than that reported for HIV-infected humans (5, 11, 13).

In most of the monkeys the T cell data are best fitted with models lacking proliferation (i.e., with the $\alpha\delta$ or the δ model). Fitting with $\rho = 0$ should not be interpreted as evidence against T cell proliferation in these monkeys (30). Because total cell numbers remain at steady state, the total production of cells should always balance the average death rate $\hat{\delta}$ in Table I, even if $\rho = 0$. Fitting with $\rho = 0$ could mean that most of the proliferation in T cells occurs during a clonal expansion involving so many divisions that labeled cells dilute their BrdU and appear as an unlabeled source (30, 32). This is one of the reasons why one can only reliably estimate an average turnover rate from these data (30).

Naive and memory T cells

Typical examples of BrdU labeling in naive and memory $CD4^+$ and $CD4^-$ T cells from the SIV-infected macaque H1348 and uninfected macaque U1426 are given in Fig. 3. The labeling of the total T cell population from these same macaques was illustrated in Fig. 2.

The naive and memory $CD4^+$ T cell data from the uninfected macaque in Fig. 3*b* show that the naive compartment has a slower accumulation of BrdU than the memory compartment, and that it remains increasing well beyond the third week of BrdU administration (for this particular monkey we fitted an unexpectedly large

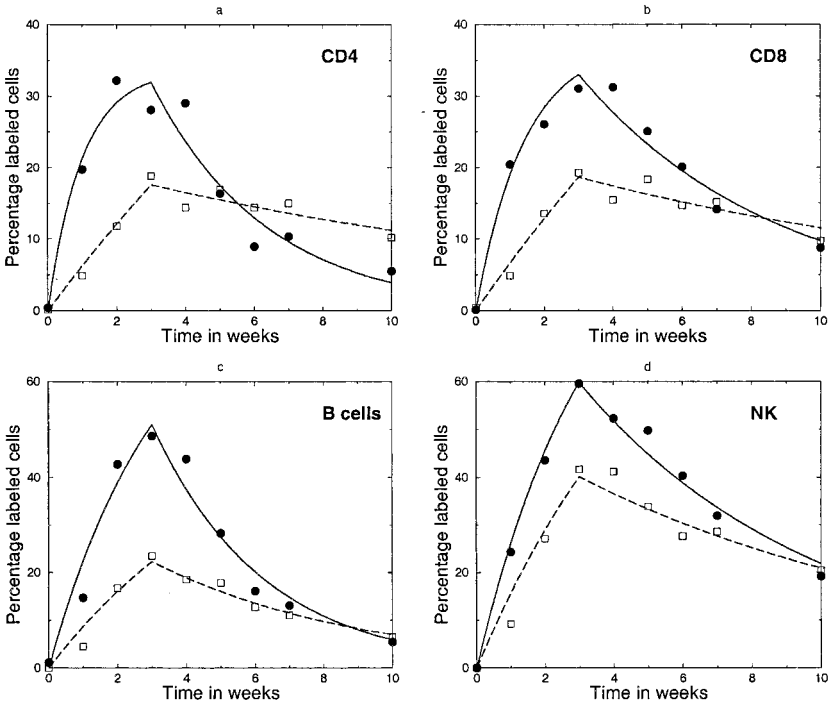

FIGURE 2. Examples of the nonlinear least squares fits of the model (lines) to the data for $CD4^+$ T cells (*a*), $CD8^+$ T cells (*b*), B cells (*c*), and NK cells (*d*) for the infected monkey H1348 and the uninfected monkey U1426, respectively. ●, The infected monkey H1348; □, the uninfected monkey U1426. Parameters in *a*: $\delta = 0.009$ per day (d^{-1}), $\alpha = 0.34$, $\rho = 0.05 d^{-1}$ (for H1348), and $\delta = 0.009 d^{-1}$ (for U1426); in *b*: $\delta = 0.063 d^{-1}$, $\alpha = 0.38$, $\rho = 0.038 d^{-1}$ (for H1348), and $\delta = 0.009 d^{-1}$ (for U1426); in *c*: $\delta = 0.044 d^{-1}$, $\alpha = 0.84$ (for H1348), and $\delta = 0.024 d^{-1}$ and $\alpha = 0.57$ (for U1426); and in *d*: $\delta = 0.032 d^{-1}$, $\rho = 0.011 d^{-1}$ (for H1348), and $\delta = 0.019 d^{-1}$ and $\rho = 0.006 d^{-1}$ (for U1426). Data from Tables I and IV.

Table I. *Average death rate of T cells*[a]

ID	Average Death Rate $\hat{\delta}$ (d^{-1}) of T Cells (×100)			
	$CD3^+CD4^+$	Model	$CD3^+CD4^-$	Model
H1284	2.1 (1.8–2.4)	δ	2.6 (2.3–3.0)	δ
H1296	1.4 (1.1–2.0)	$\alpha\rho\delta$	1.3 (1.0–1.8)	$\alpha\rho\delta$
H1314	0.9 (0.7–1.1)	δ	1.5 (1.1–1.7)	δ
H1316	1.9 (1.7–2.4)	$\alpha\rho\delta$	2.6 (2.4–2.8)	$\alpha\delta$
H1348	3.1 (2.4–5.2)	$\alpha\rho\delta$	2.4 (2.0–3.1)	$\alpha\rho\delta$
H1442	2.2 (1.8–2.7)	$\alpha\delta$	2.4 (2.0–2.8)	$\alpha\delta$
Mean	1.9 ± 0.8		2.1 ± 0.6	
L1294	1.2 (1.0–1.4)	δ	1.3 (1.1–1.4)	δ
L1324	1.2 (1.1–1.3)	$\alpha\rho\delta$	1.7 (1.5–2.0)	$\alpha\rho\delta$
L1380	0.9 (0.8–1.1)	$\alpha\delta$	0.8 (0.7–0.9)	$\alpha\delta$
L1394	0.8 (0.7–1.0)	$\alpha\delta$	0.9 (0.8–1.1)	$\alpha\delta$
L1436	2.7 (2.2–3.3)	$\alpha\delta$	1.8 (1.6–2.0)	$\alpha\delta$
Mean	1.4 ± 0.8		1.3 ± 0.5	
U1372	0.5 (0.4–0.6)	$\rho\delta$	0.8 (0.7–0.8)	δ
U1426	0.9 (0.8–1.0)	δ	1.0 (0.9–1.1)	δ
U1458	1.0 (0.9–1.1)	δ	1.3 (1.1–1.5)	$\rho\delta$
U1466	1.2 (1.1–1.3)	δ	1.2 (1.1–1.3)	δ
Mean	0.9 ± 0.3		1.1 ± 0.2	

[a] The average death rate, $\hat{\delta}$, of $CD4^+$ T cells, and $CD3^+CD4^-$ "$CD8^+$" T cells in SIV-infected and uninfected rhesus macaques. Entries in parentheses denote 95% confidence limits. Monkeys are divided into groups with a high (H) viral load, a low (L) viral load, and those that were uninfected (U). We have fitted the data to four models: the full three parameter model ($\alpha\rho\delta$), the two parameter model lacking proliferation ($\alpha\delta$), the two parameter model lacking the asymptote ($\rho\delta$), and the one parameter model (δ), respectively. From the parameter estimates of the most appropriate model, i.e., the model with the lowest residual mean square, we calculate the average death rate (30). Monkey H1314 had only 2 wk of BrdU labeling, and was fitted with t_e = 14 days.

Table II. *Average death rate of "memory" T cells*[a]

ID	Average Death Rate δ (d^{-1}) of Memory T Cells (×100)			
	$CD4^+CD45RA^-$	Model	$CD4^-CD45RA^-$	Model
H1284	3.2 (2.6–4.0)	$\alpha\delta$	3.7 (3.0–4.6)	δ
H1296	3.5 (1.7–63.0)	$\alpha\rho\delta$	2.0 (1.6–2.5)	$\alpha\delta$
H1314	2.0 (1.1–4.4)	$\alpha\delta$	1.6 (1.1–2.4)	$\alpha\delta$
H1316	4.8 (4.3–5.4)	$\alpha\rho\delta$	4.9 (3.9–5.5)	δ
H1348	3.7 (2.9–6.5)	$\alpha\rho\delta$	3.3 (2.8–4.2)	$\alpha\rho\delta$
H1442	2.4 (1.9–3.0)	$\alpha\delta$	2.6 (2.0–3.4)	$\alpha\delta$
Mean	3.3 ± 1.0		3.0 ± 1.2	
L1294	1.2 (0.9–1.4)	$\alpha\delta$	1.7 (1.4–2.1)	$\alpha\delta$
L1324	0.8 (0.7–0.8)	δ	2.4 (2.2–2.8)	$\alpha\rho\delta$
L1380	1.2 (1.0–1.4)	$\alpha\delta$	2.0 (1.5–5.3)	$\alpha\rho\delta$
L1394	0.9 (0.8–1.1)	$\alpha\delta$	1.5 (1.2–1.9)	$\alpha\delta$
L1436	3.4 (2.7–4.1)	$\alpha\delta$	2.9 (2.4–3.4)	$\alpha\delta$
Mean	1.5 ± 1.1		2.1 ± 0.6	
U1372	0.7 (0.7–0.8)	δ	1.2 (1.1–1.4)	$\alpha\delta$
U1426	0.9 (0.9–1.0)	δ	1.0 (1.0–1.1)	$\alpha\delta$
U1458	1.1 (1.0–1.1)	δ	1.0 (0.8–1.2)	$\rho\delta$
U1466	1.5 (1.3–1.7)	$\alpha\delta$	1.4 (1.2–1.6)	$\alpha\delta$
Mean	1.0 ± 0.3		1.1 ± 0.2	

[a] The average death rate $\hat{\delta}$ of $CD4^+CD45RA^-$ and $CD4^-CD45RA^-$ "memory" T cells. See Table I legend.

t_e = 54 days). The naive and memory T cell dynamics in the $CD4^-$ T cells of the uninfected macaque are much more similar (see Fig. 3*d*). Fig. 3, *a* and *c* suggest that SIV infection increases cellular turnover in both the naive and memory compartments.

The turnover rate of naive and memory $CD4^+$ T cells in uninfected macaques is 0.6 and 1.0% per day, respectively (Tables II and III). Our estimate that the turnover rate in memory $CD4^+$ T cells is only 2-fold higher than that in naive $CD4^+$ T cells is relatively low (5, 11, 13, 38). In the $CD4^-$ T cell population there seems to be no difference in turnover between the naive and memory cells (see Tables II and III). This is in disagreement with other data (5, 11, 38), and may be due to the poor characterization of naive and memory T cells by the mere absence or presence of the CD45RA Ag (39). If in rhesus monkeys the $CD45RA^+$ subpopulation of T cells is contaminated with Ag-experienced cells having a higher turnover than true naive T cells, we may indeed be underestimating the difference in naive and memory T cell turnover.

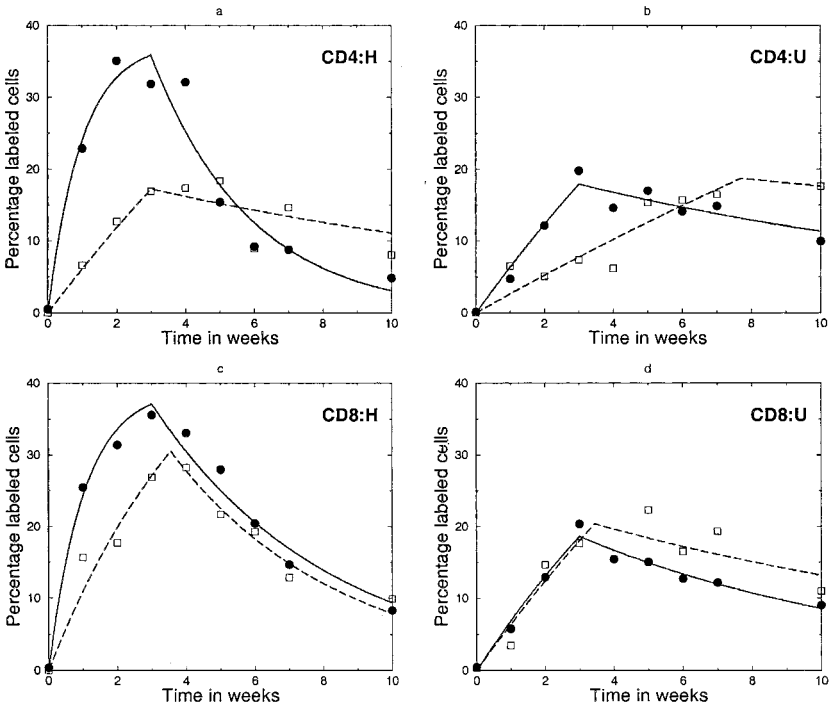

FIGURE 3. Examples of the best fits of the model for naive (dashed line) and memory T cells (solid line) in the infected monkey H1348 and the uninfected monkey U1426. The $CD4^+$ T cells are depicted for monkey H1348 (*a*) and U1426 (*b*). The $CD4^-$ T cells are depicted for monkey H1348 (*c*) and U1426 (*d*). ●, RA^- "memory" T cells; □, RA^+ "naive" T cells. Data from Table II and Table III. Parameters in *a*: $\delta = 0.098d^{-1}$, $\alpha = 0.38$, $\rho = 0.048d^{-1}$ (for RA^-) and $\delta = 0.009$ (for RA^+); in *b*: $\delta = 0.009d^{-1}$ (for RA^-) and $\delta = 0.004d^{-1}$ and t_e = 54 days (for RA^+); in *c*: $\delta = 0.083d^{-1}$, $\alpha = 0.39$, $\rho = 0.055d^{-1}$ (for RA^-) and $\delta = 0.03$, $\alpha = 0.58$, t_e = 25 (for RA^+); and in *d*: $\delta = 0.015d^{-1}$ and $\alpha = 0.66$ (for RA^-) and $\delta = 0.009d^{-1}$ and t_e = 24 days (for RA^+).

Table III. *Average death rate of "naive" T cells*[a]

ID	Average Death Rate $\hat{\delta}$ (d^{-1}) of Naive T Cells (×100)					
	$CD4^+CD45RA^+$	t_e	Model	$CD4^-CD45RA^+$	t_e	Model
H1284	1.7 (1.5–1.8)	26	$\alpha t_e\delta$	2.1 (2.0–2.3)	31	$\alpha t_e\delta$
H1296	0.8 (0.5–1.2)	21	$\alpha\delta$	1.0 (0.8–1.2)	21	$\alpha\delta$
H1314	0.5 (0.5–0.6)	21	δ	1.0 (0.8–1.1)	21	δ
H1316	1.4 (1.2–1.6)	25	$t_e\delta$	1.8 (1.7–1.9)	24	$\alpha t_e\delta$
H1348	1.0 (0.8–1.2)	21	$\alpha\delta$	1.7 (1.5–2.0)	25	$\alpha t_e\delta$
H1442	2.2 (1.7–3.1)	27	$t_e\delta$	1.7 (1.6–1.8)	21	$\alpha\delta$
Mean	1.2 ± 0.6			1.5 ± 0.5		
L1294	1.3 (1.0–1.7)	25	$t_e\delta$	1.2 (0.9–1.4)	23	$t_e\delta$
L1324	0.6 (0.5–0.8)	25	$t_e\delta$	1.8 (1.6–1.9)	21	$\alpha\delta$
L1380	0.6 (0.5–0.7)	21	$\alpha\delta$	0.6 (0.6–0.7)	21	$\alpha\delta$
L1394	0.7 (0.5–0.8)	30	$\alpha t_e\delta$	0.8 (0.7–0.8)	21	δ
L1436	1.5 (1.2–1.7)	21	$t_e\delta$	1.2 (1.1–1.3)	21	δ
Mean	0.9 ± 0.4			1.1 ± 0.4		
U1372	0.6 (0.5–0.7)	33	$t_e\delta$	0.4 (0.4–0.5)	31	$t_e\delta$
U1426	0.4 (0.3–0.5)	54	$t_e\delta$	0.9 (0.7–1.3)	25	$t_e\delta$
U1458	0.6 (0.5–0.7)	28	$t_e\delta$	2.2 (2.0–2.5)	21	δ
U1466	0.8 (0.7–0.9)	31	$t_e\delta$	1.1 (0.9–1.3)	25	$t_e\delta$
Mean	0.6 ± 0.2			1.1 ± 0.8		

[a] The average death rate $\hat{\delta}$ of $CD4^+CD45RA^+$ and $CD4^-CD45RA^+$ "naive" T cells. The data was fitted neglecting proliferation, i.e., by fixing $\rho = 0$, and allowing the parameter t_e to be free. The data was fitted to the three parameter model ($\alpha t_e\delta$), the two parameter model fixing $t_e = 21$ days ($\alpha\delta$), the two parameter model lacking the asymptote ($t_e\delta$), and the one parameter model (δ), respectively. See also the Table I legend.

SIV infection increases memory cell turnover ~3-fold in both the $CD4^+$ and the $CD4^-$ compartment (see Table II). In the $CD4^+$ compartment, the naive T cell turnover is almost 2-fold increased in monkeys with a high viral load (see Table III). For $CD4^-CD45RA^+$ T cells there is hardly any increase in the average turnover in SIV-infected monkeys (see Table III). Most of the memory T cell data are again fitted best with models lacking proliferation (i.e., the $\alpha\delta$ and the δ models).

B cells and NK cells

The average turnover of $CD3^-CD20^+$ "B cells" and $CD3^-CD8^+$ CD16+ "NK cells" in the four uninfected monkeys is ~2% per day (Table IV). This may be biased by the high turnover in monkey U1458, whom at week four has peak values of 55 and 29% $BrdU^+$ B cells and NK cells, respectively. This monkey had an unexpectedly low CD4 count in the peripheral blood (4), and it was later found that he died of hepatic degeneration associated with cachexia and wasting due to loss of gastrointestinal tract function. Excluding U1458, we obtain daily turnover rates of 1.8 ± 0.6 and 1.6 ± 0.6, for the B cell and NK cell averages, respectively. The daily turnover rates of B cells and NK cells are increased to 3 and 2.5%, respectively, in infected monkeys with a high viral load. In infected monkeys with a low viral load, the turnover rate is actually smaller than that in uninfected monkeys (which could be due to the aberrant uninfected monkey U1458). Thus, SIV infection also increases the cellular turnover of B cells and NK cells, albeit to a lower extend than in T cells. This confirms earlier observations (40).

The B cell data are typically fitted best with a source/death model (i.e., in Table IV, 12 of 15 cases are best fitted with the $\alpha\delta$ model in which $\rho = 0$). This would be in agreement with an interpretation of considerable B cell production by the bone marrow and/or by considerable clonal expansion (30). Conversely, the NK cell data require a nonzero proliferation in 11 of the 15 cases (see Table IV). The two typical examples depicted in Fig. 2 indeed confirm that the NK cell data tend to have different slopes during the labeling and delabeling period, whereas the two slopes of the B cells are similar. Therefore, the NK cell data seem to suggest that the maintenance of NK cells involves proliferation in the form of peripheral renewal (30).

Immune activation

Decreasing the CD4 T cell count in the peripheral blood tends to increase cellular turnover for all cell types studied here (Figs. 4 and 5). Although, similar data have been published before for T cells (4, 5, 13, 18), these correlations might not reflect cause and effect because the CD4 T cell count is typically correlated negatively with the viral load (13, 18). For the current data we also find a negative relation between the viral load and the CD4 count (Fig.

Table IV. *Average death rate of "B" and "NK" cells*[a]

ID	Average Death Rate $\hat{\delta}$ (d^{-1}) of B and NK Cells (×100)			
	$CD3^-CD20^+$	Model	$CD3^-CD8^+CD16^+$	Model
H1284	2.0 (1.6–2.6)	$\alpha\delta$	3.4 (3.2–4.1)	$\rho\delta$
H1296	1.5 (1.3–1.7)	$\alpha\delta$	1.8 (1.4–2.7)	$\alpha\rho\delta$
H1314	2.7 (1.2–4.9)	$\alpha\delta$	2.9 (2.0–4.0)	$\rho\delta$
H1316	4.7 (4.1–5.9)	$\alpha\rho\delta$	2.7 (2.6–2.9)	$\rho\delta$
H1348	3.7 (3.2–4.3)	$\alpha\delta$	3.2 (2.9–3.5)	$\rho\delta$
H1442	3.5 (2.7–4.4)	δ	1.9 (1.3–2.7)	$\alpha\delta$
Mean	3.0 ± 1.2		2.6 ± 0.7	
L1294	1.5 (1.0–2.0)	$\alpha\delta$	2.0 (1.6–2.4)	$\rho\delta$
L1324	2.4 (1.9–2.8)	$\alpha\delta$	2.1 (1.9–2.3)	$\rho\delta$
L1380	1.3 (1.1–1.4)	$\alpha\delta$	1.1 (1.0–1.2)	δ
L1394	1.8 (1.4–2.2)	$\alpha\delta$	1.5 (1.2–1.8)	δ
L1436	2.0 (1.5–2.5)	$\alpha\delta$	2.0 (1.6–2.4)	$\rho\delta$
Mean	1.8 ± 0.4		1.7 ± 0.4	
U1372	1.5 (1.3–1.7)	$\alpha\delta$	0.9 (0.6–1.2)	$\rho\delta$
U1426	1.4 (1.1–1.5)	$\alpha\delta$	1.9 (1.5–2.2)	$\rho\delta$
U1458	3.5 (2.9–5.0)	$\alpha\rho\delta$	2.6 (2.2–2.9)	$\rho\delta$
U1466	2.4 (1.9–3.1)	$\alpha\delta$	2.1 (1.7–2.4)	$\rho\delta$
Mean	2.2 ± 1.0		1.9 ± 0.7	

[a] The average death rate, $\hat{\delta}$, of $CD3^-CD20^+$ "B cells" and $CD3^-CD8^+CD16^+$ "NK cells" in SIV-infected and uninfected rhesus macaques. See the Table I legend.

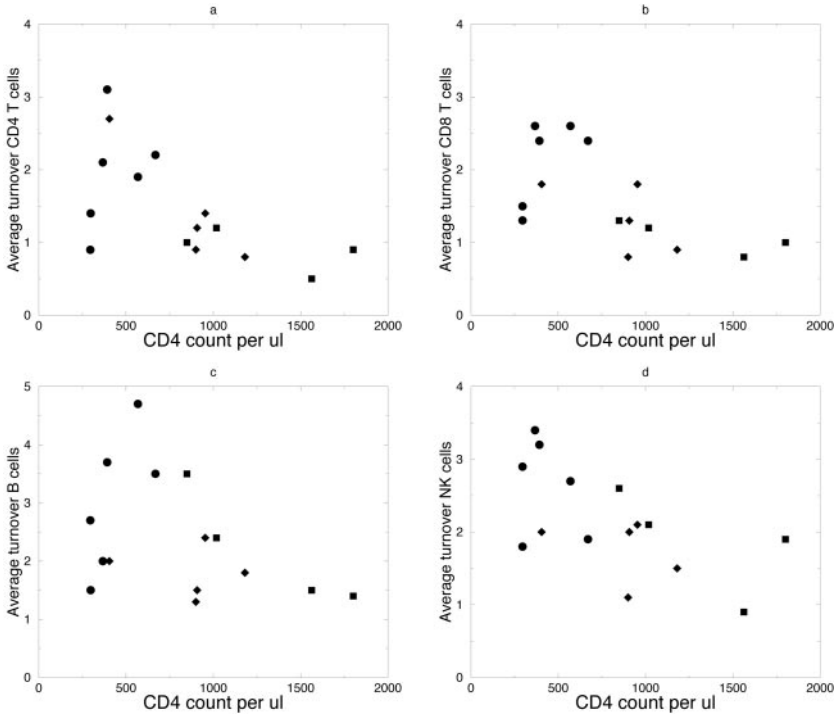

FIGURE 4. The average death rates $\hat{\delta}$ of $CD4^+$ T cells (*a*), $CD4^-$ T cells (*b*), B cells (*c*), and NK cells (*d*), as a function of the CD4 T cell count per microliter of peripheral blood. The correlation coefficients in *a–d* are $r = -0.63$, $r- = 0.63$, $r = -0.40$, $r = -0.61$ ($n = 15$), respectively. Data from Tables I and IV and Mohri et al. (4).

6*d*). Different studies disagree on the relative contribution of the viral load and the CD4 T cell count on immune activation: Cohen Stuart et al. (18) find that both have a partial contribution, Lempicki et al. (13) find no true effect of CD4 T cell count, and Leng et al. (41) find that the CD4 T cell count has the largest contribution.

Whatever the underlying mechanism, the data definitely demonstrate that with decreasing CD4 T cell counts many different cell types have an increased cellular turnover. This suggests that there is a common mechanism increasing cellular turnover when CD4 counts are low. We indeed find that the turnover rates within each monkey are highly correlated. Fig. 6 shows that the turnover rates of $CD4^-$ T cells, B cells, and NK cells are correlated with the estimated turnover rate of the $CD4^+$ T cells, although the turnover of B cells and NK cells tends to be faster than that of the T cells.

Although one could argue that a $CD4^+$ T cell homeostatic response to low CD4 T cell counts could up-regulate cellular turnover in various cell types, it seems more likely that the common factor correlated with the CD4 T cell count is a global immune activation associated with viral Ags and/or other infections (11, 13, 18, 41–44). Supporting evidence for this is the rapid decrease in cellular turnover in patients on anti-retroviral therapy long before the CD4 T cell counts have normalized (11, 13, 31).

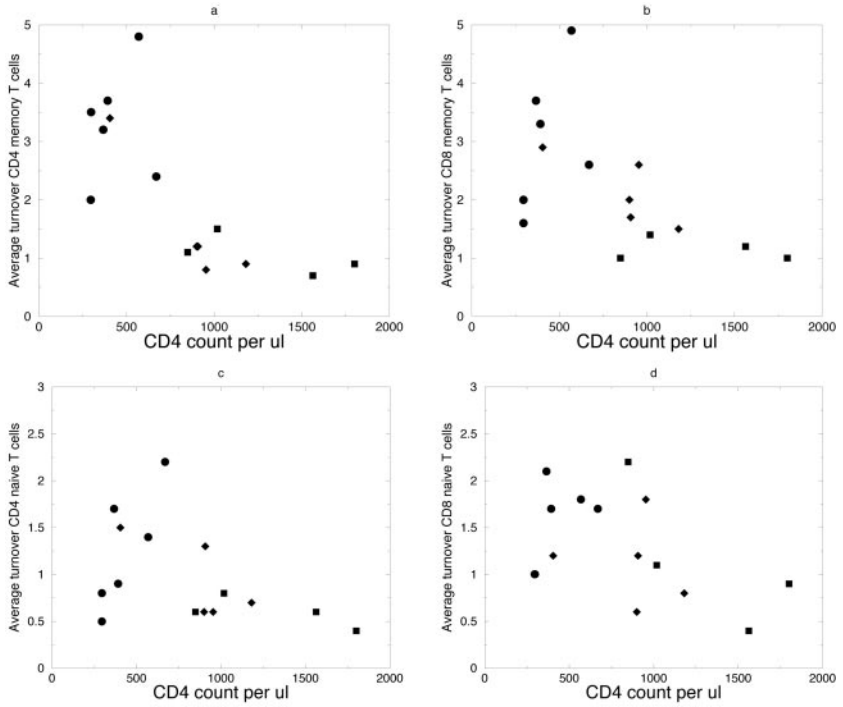

FIGURE 5. The average death rates of naive and memory T cells. The four panels depict $100 \times \hat{\delta}$ of $CD4^+RA^-$ T cells (*a*), $CD4^-RA^-$ T cells (*b*), $CD4^+RA^+$ T cells (*c*), and $CD8^+RA^+$ T cells (*d*), as a function of the CD4 T cell count per microliter of peripheral blood. The correlation coefficients in *a–d* are $r = -0.74$, $r- = 0.58$, $r = -0.45$, $r = -0.46$ ($n = 15$), respectively. Data from Tables II and III and Mohri et al. (4).

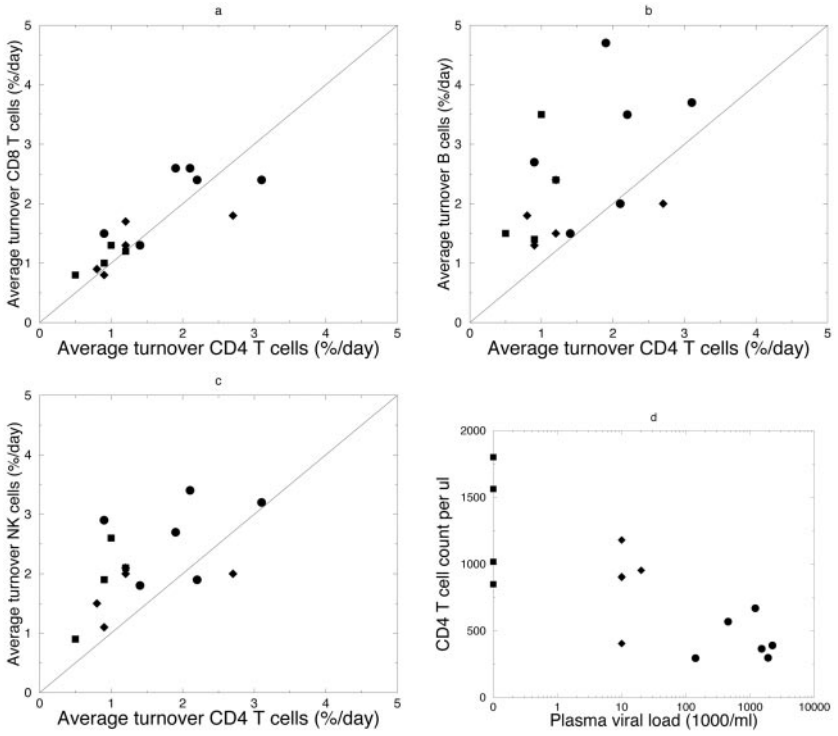

FIGURE 6. The average death rates $100 \times \hat{\delta}$ of $CD8^+$ T cells (*a*), B cells (*b*), and NK cells (*c*), as a function of the average death rate of $CD4^+$ T cells (data from Tables I and IV). The correlation coefficients in *a–c* are $r = 0.81$, $r = 0.48$, and $r = 0.56$, respectively ($n = 15$). *d*, The CD4 T cell count per microliter of peripheral blood as a function of the plasma viral load, (which can be zero (uninfected macaques) or undetectable, i.e., <10) (data from Mohri et al. (4)).

Discussion

Using BrdU labeling and nonlinear least squares fitting of the measured fraction of labeled cells vs time (labeling curves) to simple models of lymphocyte dynamics has allowed us to estimate parameters characterizing lymphocyte turnover in SIV^- and SIV^+ macaques. As explained in the companion paper (30), here we estimate the average turnover rate of various lymphocyte subpopulations, where the average turnover rate is defined as the average death rate of the whole population being sampled for $BrdU^+$ cells. Previously, using a subset of the data analyzed in this study, we estimated the death rate, δ, of the $CD4^+$ and $CD8^+$ T cell populations (4). However, the death rate estimated in Ref. 4 applied only to the subpopulation of activated $CD4^+$ and $CD8^+$ T cells, and not the entire population (30, 45).

The estimates of the average turnover rate, $\hat{\delta}$, provided in Tables I-III have somewhat narrower 95% confidence limits than the previously published estimates of δ. The reason for this is 2-fold. First, the average turnover rate is sensitive to events in both activated and resting cell populations and hence depends less on the detailed assumptions made about these subpopulations. Because activation and division of resting cells acts as a source of proliferating cells various tradeoffs among parameters can occur when matching experimental data. Because the average turnover rate hardly changes when these tradeoffs occur (30), we obtain better confidence limits on its estimate. Second, we use a statistical procedure to fit each data set with a model having the minimal number of parameters required to explain the data. This also narrows the confidence limits (30). These two improvements enable us to draw more reliable conclusions about T lymphocyte turnover in SIV^- and SIV^+ macaques, and to analyze data on additional subsets of cells.

The nature of the source is clearly of biological interest. The data that we obtain from BrdU labeling cannot fully define the source. However, we have previously shown (29) that we can replace the source by a population of resting cells that upon activation enters the proliferating compartment. Our published detailed analysis of this model shows that if the resting cells are truly resting, or if they divide very slowly compared with the rate of division of the activated cells, then one recovers a model with a constant source. In addition, we have recently analyzed ^{2}H-glucose labeling data in humans using models with a constant source (31) and with models without a source but with a resting population that becomes activated (46, 47) and have shown that both models yield the same estimates for activated cell death rates. Finally, we have argued that BrdU dilution by clonal expansion provides an explanation for the source of unlabeled cells after BrdU withdrawal (32), and have shown that under these different interpretations our procedure of fitting an average turnover rate yields similar estimates (30). Thus, we have reasonable confidence that the nature of the source will not change our conclusions about the proliferating pool of cells.

We have found that monkeys with low $CD4^+$ T cell counts tend to have higher average turnover rates in $CD45RA^+$ "naive" and $CD45RA^-$ "memory" $CD4^+$ and $CD4^-$ T cell populations, in $CD3^-CD20^+$ B cells, and in $CD3^-CD8^+CD16+$ NK cells. Thus, the turnover rates in the various populations are correlated positively, which suggest that generalized immune activation is driving the increased turnover. Moreover, because $CD4^+$ T cell counts and viral loads are negatively correlated, increased immune activation could also be due to increased viral loads. In this data, the increase in average cellular turnover rates caused by SIV infection is typically <2-fold. This level of increase in cellular turnover is in good agreement with telomere data showing little effect of HIV infection on the average telomere length in naive and memory $CD4^+$ T cells (17, 48), and with TCR rearrangement excision circle data showing a decrease in the TCR rearrangement excision circles per naive T cell in response to a small increase in the division rate (49).

Our estimated 2-fold increase in cellular turnover with SIV infection is smaller than estimates in HIV-1-infected humans obtained with the Ki67 mAb (5, 11, 13), or with ^{2}H-glucose labeling (10, 31). Because the average turnover rate depends on the $CD4^+$ T cell count (see Fig. 4), this is probably due to differences in the

disease stage of the subjects in the various studies. Human patients with high $CD4^+$ T cell counts have low fractions of $Ki67^+$ T cells (8), whereas patients with low counts have high fractions of $Ki67^+$ T cells (5, 11). Importantly, Ki67 data from Chakrabarti et al. (50) show that rhesus macaques naturally have a high percentage of T cells in division, i.e., 7% of the $CD4^+$ T cells are $Ki67^+$ and 7.8% of the $CD8^+$ T cells, and that these percentages increase 2- to 3-fold upon SIV infection (50). Thus, the difference between the two studies in the fold-increase caused by the infection, i.e., 6-fold in humans and 2-fold in macaques, could be largely due to our higher estimated average turnover rate in healthy macaques. Additionally, there could be a methodological problem with Ki67. The Ki67 mAb labels cells during the late G_1, M, and S phases of the cell cycle (51). However, nondividing activated cells remaining in the G_1 phase may be $Ki67^+$ (52, 53). In contrast to normal individuals, a large fraction of the $CD4^+CD45RO^+Ki67^+$ T cells in HIV-infected patients are in the G_1 phase of the cell cycle (53). Another study found that both in healthy controls and in HIV-1-infected patients, >40% of the $Ki67^+CD4^+$ T cells express CTLA-4, suggesting that these cells were not proliferating, whereas only 20% of the $Ki67^+CD8^+$ T cells were CTLA-4^+ (41). To resolve this discrepancy between Ki67 measurements and cellular proliferation we need a method of translating Ki67 measurements into the corresponding proliferation rates. The excellent positive correlation between the fraction of $Ki67^+$ cells and the estimated proliferation rate of $CD4^+$ and $CD8^+$ T cells in HIV-1-infected patients and healthy human controls labeled with ^{2}H-glucose (31), suggests that such a translation is feasible.

BrdU labeling was recently applied to human HIV-1-infected patients (14). Because the authors fit a phenomenological model to the data, the comparison to our results is difficult. First, the authors find that during the delabeling phase the loss of the labeled fraction is biphasic, and therefore fit two exponential slopes. These slopes are interpreted as the death rates of two distinct subpopulations. However, from the more mechanistic models derived in this study and before (4, 29, 30) we know that the down slope reflects the difference between the rates of death and proliferation, rather than the death rate alone. This complicates matters substantially because the result that the phenomenological death rate is not affected by therapy (14) could mean that both proliferation (13) and death decrease during therapy, and that their difference remains similar. Second, the authors find that the percentage of labeled cells correlates positively with the plasma viral load, and that it decreases with treatment (14). This percentage attained after 30 min in vivo pulse labeling with BrdU should be proportional to what we call the average turnover rate. The higher the average turnover within a population the higher the fraction of labeled cells after a pulse labeling. Such an interpretation would allow for an agreement between the results because we find that the average turnover rate of various cell types correlates negatively with $CD4^+$ T cell counts, which are inversely related to the plasma viral load.

If SIV/HIV infection increases the cellular turnover in various cell types, the obvious question is why are only the $CD4^+$ T cell counts depleted by these lentiviruses. However, this question should be addressed carefully because HIV-1 infection differentially affects various lymphocyte subpopulations. For instance, the total $CD8^+$ T cell population increases, but the naive $CD8^+$ T cell subcompartment is depleted by HIV-1 infection (15, 16). There is evidence that the Th2-type immune activation caused by chronic helminth infections leads to decreased $CD4^+$ T cell counts and increased $CD8^+$ T cell counts (54), and the chronic immune activation associated with rheumatoid arthritis exhausts the T cell repertoire (without depleting naive or memory $CD4^+$ T cell, however) (2). It remains unclear whether these other systems can be extrapolated to HIV-1 infection. Moreover, these observations still fail to explain why $CD4^+$ T cells would be more vulnerable to chronic activation than other cell types. One obvious difference between $CD4^+$ T cells and other cell types in HIV infection is that HIV infects $CD4^+$ T cells, which as a consequence may die, or be cleared by the immune response. However, because only a small fraction, i.e., 0.1% or less, of all $CD4^+$ T cells are productively infected at any given time (55–57), this explanation remains unsatisfying (58, 59) and needs further quantitative elaboration.

Acknowledgments

We thank José Borghans, Can Keşmir, and Ruy Ribeiro for helpful discussions. We thank Cas Kruitwagen for statistical advice.

References

1. Wagner, U. G., K. Koetz, C. M. Weyand, and J. J. Goronzy. 1998. Perturbation of the T cell repertoire in rheumatoid arthritis. *Proc. Natl. Acad. Sci. USA 95: 14447.*
2. Koetz, K., E. Bryl, K. Spickschen, W. M. O'Fallon, J. J. Goronzy, and C. M. Weyand. 2000. T cell homeostasis in patients with rheumatoid arthritis. *Proc. Natl. Acad. Sci. USA 97:9203.*
3. Ho, D. D., A. U. Neumann, A. S. Perelson, W. Chen, J. M. Leonard, and M. Markowitz. 1995. Rapid turnover of plasma virions and CD4 lymphocytes in HIV-1 infection. *Nature 373:123.*
4. Mohri, H., S. Bonhoeffer, S. Monard, A. S. Perelson, and D. D. Ho. 1998. Rapid turnover of T lymphocytes in SIV-infected rhesus macaques. *Science 279:1223.*
5. Sachsenberg, N., A. S. Perelson, S. Yerly, G. A. Schockmel, D. Leduc, B. Hirschel, and L. Perrin. 1998. Turnover of $CD4^+$ and $CD8^+$ T lymphocytes in HIV-1 infection as measured by Ki-67 antigen. *J. Exp. Med. 187:1295.*
6. Zhang, Z. Q., D. W. Notermans, G. Sedgewick, W. Cavert, S. Wietgrefe, M. Zupancic, K. Gebhard, K. Henry, L. Boies, Z. Chen, et al. 1998. Kinetics of $CD4^+$ T cell repopulation of lymphoid tissues after treatment of HIV-1 infection. *Proc. Natl. Acad. Sci. USA 95:1154.*
7. Rosenzweig, M., M. DeMaria, D. M. Harper, S. Friedrich, R. K. Jain, and R. P. Johnson. 1998. Increased rates of $CD4^+$ and $CD8^+$ T lymphocyte turnover in simian immunodeficiency virus-infected macaques. *Proc. Natl. Acad. Sci. USA 95:6388.*
8. Fleury, S., R. J. De Boer, G. P. Rizzardi, K. C. Wolthers, S. A. Otto, C. C. Welbon, C. Graziosi, C. Knabenhans, H. Soudeyns, P. A. Bart, et al. 1998. Limited $CD4^+$ T-cell renewal in early HIV-1 infection: effect of highly active antiretroviral therapy. *Nat. Med. 4:794.*
9. Clark, D. R., R. J. De Boer, K. C. Wolthers, and F. Miedema. 1999. T cell dynamics in HIV-1 infection. *Adv. Immunol. 73:301.*
10. Hellerstein, M., M. B. Hanley, D. Cesar, S. Siler, C. Papageorgopoulos, E. Wieder, D. Schmidt, R. Hoh, R. Neese, D. Macallan, et al. 1999. Directly measured kinetics of circulating T lymphocytes in normal and HIV-1-infected humans. *Nat. Med. 5:83.*
11. Hazenberg, M. D., J. W. Cohen Stuart, S. A. Otto, J. C. Borleffs, C. A. Boucher, R. J. De Boer, F. Miedema, and D. Hamann. 2000. T-cell division in human immunodeficiency virus (HIV)-1 infection is mainly due to immune activation: a longitudinal analysis in patients before and during highly active antiretroviral therapy (HAART). *Blood 95:249.*
12. McCune, J. M., M. B. Hanley, D. Cesar, R. Halvorsen, R. Hoh, D. Schmidt, E. Wieder, S. Deeks, S. Siler, R. Neese, and M. Hellerstein. 2000. Factors influencing T-cell turnover in HIV-1-seropositive patients. *J. Clin. Invest. 105:R1.*
13. Lempicki, R. A., J. A. Kovacs, M. W. Baseler, J. W. Adelsberger, R. L. Dewar, V. Natarajan, M. C. Bosche, J. A. Metcalf, R. A. Stevens, L. A. Lambert, et al. 2000. Impact of HIV-1 infection and highly active antiretroviral therapy on the kinetics of $CD4^+$ and $CD8^+$ T cell turnover in HIV-infected patients. *Proc. Natl. Acad. Sci. USA 97:13778.*
14. Kovacs, J. A., R. A. Lempicki, I. A. Sidorov, J. W. Adelsberger, B. Herpin, J. A. Metcalf, I. Sereti, M. A. Polis, R. T. Davey, J. Tavel, et al. 2001. Identification of dynamically distinct subpopulations of T lymphocytes that are differentially affected by HIV. *J. Exp. Med. 194:1731.*
15. Roederer, M., J. G. Dubs, M. T. Anderson, P. A. Raju, L. A. Herzenberg, and L. A. Herzenberg. 1995. CD8 naive T cell counts decrease progressively in HIV-infected adults. *J. Clin. Invest. 95:2061.*
16. Hazenberg, M. D., D. Hamann, H. Schuitemaker, and F. Miedema. 2000. T cell depletion in HIV-1 infection: how $CD4^+$ T cells go out of stock. *Nat. Immunol. 1:285.*
17. Wolthers, K. C., G. B. A. Wisman, S. A. Otto, A. M. De Roda Husman, N. Schaft, F. De Wolf, J. Goudsmit, R. A. Coutinho, A. G. Van der Zee, L. Meyaard, and F. Miedema. 1996. T cell telomere length in HIV-1 infection: no evidence for increased $CD4^+$ T cell turnover. *Science 274:1543.*
18. Cohen Stuart, J. W., M. D. Hazebergh, D. Hamann, S. A. Otto, J. C. Borleffs, F. Miedema, C. A. Boucher, and R. J. De Boer. 2000. The dominant source of $CD4^+$ and $CD8^+$ T-cell activation in HIV infection is antigenic stimulation. *J. Acquired Immune Defic. Syndr. 25:203.*
19. Gratzner, H. G. 1982. Monoclonal antibody to 5-bromo- and 5-iododeoxyuridine: a new reagent for detection of DNA replication. *Science 218:474.*

20. Forster, I., P. Vieira, and K. Rajewsky. 1989. Flow cytometric analysis of cell proliferation dynamics in the B cell compartment of the mouse. *Int. Immunol. 1:321.*
21. Penit, C., and F. Vasseur. 1988. Sequential events in thymocyte differentiation and thymus regeneration revealed by a combination of bromodeoxyuridine DNA labeling and antimitotic drug treatment. *J. Immunol. 140:3315.*
22. Schittek, B., and K. Rajewsky. 1990. Maintenance of B-cell memory by long-lived cells generated from proliferating precursors. *Nature 346:749.*
23. Forster, I., and K. Rajewsky. 1990. The bulk of the peripheral B-cell pool in mice is stable and not rapidly renewed from the bone marrow. *Proc. Natl. Acad. Sci. USA 87:4781.*
24. Rocha, B., C. Penit, C. Baron, F. Vasseur, N. Dautigny, and A. A. Freitas. 1990. Accumulation of bromodeoxyuridine-labeled cells in central and peripheral lymphoid organs: minimal estimates of production and turnover rates of mature lymphocytes. *Eur. J. Immunol. 20:1697.*
25. Tough, D. F., and J. Sprent. 1994. Turnover of naive- and memory-phenotype T cells. *J. Exp. Med. 179:1127.*
26. Dolbeare, F. 1995. Bromodeoxyuridine: a diagnostic tool in biology and medicine. I. Historical perspectives, histochemical methods and cell kinetics. *Histochem. J. 27:339.*
27. Zimmerman, C., K. Brduscha-Riem, C. Blaser, R. M. Zinkernagel, and H. Pircher. 1996. Visualization, characterization, and turnover of $CD8^+$ memory T cells in virus-infected hosts. *J. Exp. Med. 183:1367.*
28. Tough, D. F., and J. Sprent. 1998. Lifespan of γ/δ T cells. *J. Exp. Med. 187:357.*
29. Bonhoeffer, S., H. Mohri, D. Ho, and A. S. Perelson. 2000. Quantification of cell turnover kinetics using 5-bromo-2′-deoxyuridine. *J. Immunol. 164:5049.*
30. De Boer, R. J., H. Mohri, D. D. Ho, and A. S. Perelson. Estimating average cellular turnover from BrdU measurements. *Proc. R. Soc. London Ser. B. In press.*
31. Mohri, H., A. S. Perelson, K. Tung, R. M. Ribeiro, B. Ramratnam, M. Markowitz, R. Kost, A. Hurley, L. Weinberger, D. Cesar, et al. 2001. Increased turnover of T lymphocytes in HIV-1 infection and its reduction by antiretroviral therapy. *J. Exp. Med. 194:1277.*
32. Rouzine, I. M., and J. M. Coffin. 1999. T cell turnover in SIV infection. *Science 284:555b.*
33. Scollay, R., and D. I. Godfrey. 1995. Thymic emigration: conveyor belts or lucky dips? *Immunol. Today 16:268.*
34. Armitage, P., and G. Berry. 1994. *Statistical Methods in Medical Research*, 2nd Ed. Blackwell, Oxford.
35. Davidian, M., and D. Giltinan. 1995. Nonlinear models for repeated measurement data. In *Monographs on Statistics and Applied Probability 62*. Chapman and Hall, London.
36. Marquardt, D. W. 1963. Finite difference algorithm for curve fitting. *J. Soc. Ind. Appl. Math. 11:431.*
37. Efron, B., and R. Tibshirani. 1986. Bootstrap methods for standard errors, confidence intervals, and other measures of statistical accuracy. *Stat. Sci. 1:54.*
38. Michie, C. A., A. McLean, C. Alcock, and P. C. Beverley. 1992. Lifespan of human lymphocyte subsets defined by CD45 isoforms. *Nature 360:264.*
39. Hamann, D., P. A. Baars, M. H. Rep, B. Hooibrink, S. R. Kerkhof-Garde, M. R. Klein, and R. A. Van Lier. 1997. Phenotypic and functional separation of memory and effector human $CD8^+$ T cells. *J. Exp. Med. 186:1407.*
40. Martinez-Maza, O., E. Crabb, R. T. Mitsuyasu, J. L. Fahey, and J. V. Giorgi. 1987. Infection with the human immunodeficiency virus (HIV) is associated with an in vivo increase in B lymphocyte activation and immaturity. *J. Immunol. 138:3720.*
41. Leng, Q., G. Borkow, Z. Weisman, M. Stein, A. Kalinkovich, and Z. Bentwich. 2001. Immune activation correlates better than HIV plasma viral load with CD4 T-cell decline during HIV infection. *J. Acquired Immune Defic. Syndr. 27:389.*
42. Fauci, A. S. 1993. Multifactorial nature of human immunodeficiency virus disease: implications for therapy. *Science 262:1011.*
43. Ascher, M. S., and H. W. Sheppard. 1988. AIDS as immune system activation: a model for pathogenesis. *Clin. Exp. Immunol. 73:165.*
44. Bentwich, Z., A. Kalinkovich, Z. Weisman, and Z. Grossman. 1998. Immune activation in the context of HIV infection. *Clin. Exp. Immunol. 111:1.*
45. Asquith, B., C. Debacq, D. C. Macallan, L. Willems, and C. R. Bangham. 2002. Lymphocyte kinetics: the interpretation of labelling data. *Trends Immunol. 23: 596.*
46. Ribeiro, R. M., H. Mohri, D. D. Ho, and A. S. Perelson. 2002. Modeling deuterated glucose labeling of T-lymphocytes. *Bull. Math. Biol. 64:385.*
47. Ribeiro, R. M., H. Mohri, D. D. Ho, and A. S. Perelson. 2002. In vivo dynamics of T cell activation, proliferation, and death in HIV-1 infection: why are $CD4^+$ but not $CD8^+$ T cells depleted? *Proc. Natl. Acad. Sci. USA 99:15572.*
48. Wolthers, K. C., A. J. Noest, S. A. Otto, F. Miedema, and R. J. De Boer. 1999. Normal telomere lengths in naive and memory $CD4^+$ T cells in HIV type 1 infection: a mathematical interpretation. *AIDS Res. Hum. Retroviruses 15:1053.*
49. Hazenberg, M. D., S. A. Otto, J. W. Stuart, M. C. Verschuren, J. C. Borleffs, C. A. Boucher, R. A. Coutinho, J. M. Lange, T. F. De Wit, A. Tsegaye, et al. 2000. Increased cell division but not thymic dysfunction rapidly affects the T-cell receptor excision circle content of the naive T cell population in HIV-1 infection. *Nat. Med. 6:1036.*
50. Chakrabarti, L. A., S. R. Lewin, L. Zhang, A. Gettie, A. Luckay, L. N. Martin, E. Skulsky, D. D. Ho, C. Cheng-Mayer, and P. A. Marx. 2000. Normal T-cell turnover in sooty mangabeys harboring active simian immunodeficiency virus infection. *J. Virol. 74:1209.*
51. Bruno, S., and Z. Darzynkiewicz. 1992. Cell cycle dependent expression and stability of the nuclear protein detected by Ki-67 antibody in HL-60 cells. *Cell Prolif. 25:31.*
52. Iatropoulos, M. J., and G. M. Williams. 1996. Proliferation markers. *Exp. Toxicol. Pathol. 48:175.*
53. Combadere, B., C. Blanc, T. Li, G. Carcelain, C. Delaugerre, V. Calvez, R. Tubiana, P. Debre, C. Katlama, and B. Autran. 2000. $CD4^+$ $Ki67^+$ lymphocytes in HIV-infected patients are effector T cells accumulated in the G_1 phase of the cell cycle. *Eur. J. Immunol. 30:3598.*
54. Kalinkovich, A., Z. Weisman, Z. Greenberg, J. Nahmias, S. Eitan, M. Stein, and Z. Bentwich. 1998. Decreased CD4 and increased CD8 counts with T cell activation is associated with chronic helminth infection. *Clin. Exp. Immunol. 114: 414.*
55. Haase, A. T., K. Henry, M. Zupancic, G. Sedgewick, R. A. Faust, H. Melroe, W. Cavert, K. Gebhard, K. Staskus, Z. Q. Zhang, et al. 1996. Quantitative image analysis of HIV-1 infection in lymphoid tissue. *Science 274:985.*
56. Cavert, W., D. W. Notermans, K. Staskus, S. W. Wietgrefe, M. Zupancic, K. Gebhard, K. Henry, Z. Q. Zhang, R. Mills, H. McDade, et al. 1997. Kinetics of response in lymphoid tissues to antiretroviral therapy of HIV-1 infection. *Science 276:960.*
57. Chun, T. W., L. Carruth, D. Finzi, X. Shen, J. A. DiGiuseppe, H. Taylor, M. Hermankova, K. Chadwick, J. Margolick, T. C. Quinn, et al. 1997. Quantification of latent tissue reservoirs and total body viral load in HIV-1 infection. *Nature 387:183.*
58. Ascher, M. S., H. W. Sheppard, R. W. Anderson, J. F. Krowka, and H. J. Bremermann. 1995. HIV results in the frame: paradox remains. *Nature 375:196.*
59. Anderson, R. W., M. S. Ascher, and H. W. Sheppard. 1998. Direct HIV cytopathicity cannot account for CD4 decline in AIDS in the presence of homeostasis: a worst-case dynamic analysis. *J. Acquired Immune Defic. Syndr. Hum. Retrovirol. 17:245.*